

Theoretical Model of Superconducting Spintronic SIsFS Devices

S. V. Bakurskiy,^{1,2} N. V. Klenov,^{1,2} I. I. Soloviev,¹ V. V. Bol'ginov,³ V. V. Ryazanov,³
I. V. Vernik,⁴ O. A. Mukhanov,⁴ M. Yu. Kupriyanov,¹ and A. A. Golubov⁵

¹*Lomonosov Moscow State University Skobeltsyn Institute of Nuclear Physics (MSU SINP), Leninskie gory, GSP-1, Moscow 119991, Russian Federation*

²*Faculty of Physics, Lomonosov Moscow State University, 119992 Leninskie Gory, Moscow, Russian Federation*

³*Institute of Solid State Physics, Russian Academy of Sciences, Chernogolovka, 142432, Russian Federation*

⁴*HYPRES, Inc. 175 Clearbrook Rd., Elmsford, NY 10523 USA*

⁵*Faculty of Science and Technology and MESA+ Institute for Nanotechnology, University of Twente, 7500 AE Enschede, The Netherlands*

(Dated: 6 July 2018)

Motivated by recent progress in development of cryogenic memory compatible with single flux quantum (SFQ) circuits we have performed a theoretical study of magnetic SIsFS Josephson junctions, where 'S' is a bulk superconductor, 's' is a thin superconducting film, 'F' is a metallic ferromagnet and 'I' is an insulator. We calculate the Josephson current as a function of s and F layers thickness, temperature and exchange energy of F film. We outline several modes of operation of these junctions and demonstrate their unique ability to have large product of a critical current I_C and a normal-state resistance R_N in the π state, comparable to that in SIS tunnel junctions commonly used in SFQ circuits. We develop a model describing switching of the Josephson critical current in these devices by external magnetic field. The results are in good agreement with the experimental data for Nb-Al/ AlO_x -Nb-Pd_{0.99}Fe_{0.01}-Nb junctions.

PACS numbers: 74.45.+c, 74.50.+r, 74.78.Fk, 85.25.Cp

Practical applications of superconducting digital circuits were significantly limited by the relatively low capacity of superconducting memory. This motivated initial proposals to use superconductor/ferromagnet (S/F) hybrid structures as basis for the development in cryogenic magnetic Random Access Memories (RAMs)¹⁻³. Following the first experimental realization of SFS Josephson junctions^{4,5}, much attention was paid to realize Josephson devices with complex magnetic barriers allowing switching between high and low critical currents. A number of different device structures were considered⁶⁻¹⁴ based either on superconducting spintronics effects or singlet-triplet switching within the magnetic barrier. However, these approaches were based on structures with reduced characteristic voltage $I_c R_N$ of junctions.

Recently, successful realization of switchable Nb-Al/ AlO_x -Nb-Pd_{0.99}Fe_{0.01}-Nb junctions was reported in¹⁵⁻¹⁷. These junctions are of SIsFS type, i.e., a serial connection of the SIs tunnel junction and sFS sandwich. SIsFS structure has high characteristic voltage, $I_c R_N$, due to the presence of tunnel barrier 'I'. At the same time the whole structure behaves as a single junction with respect to an external magnetic field H_{ext} and magnetic flux Φ penetrating into the structure, since the intermediate layer s is too thin to screen magnetic field. As a result, the magnetic field entering the Pd_{0.99}Fe_{0.01} layer will modify its effective magnetization, facilitating the critical current control of the whole double-barrier SIsFS structure. According to Ref.¹⁸, effective magnetization in the dilute Pd_{0.99}Fe_{0.01} is controlled by Fe-rich Pd₃Fe nanoclusters, which can be easily reordered by a weak magnetic field. The purpose of this paper is to develop a theory describing various modes of operation of

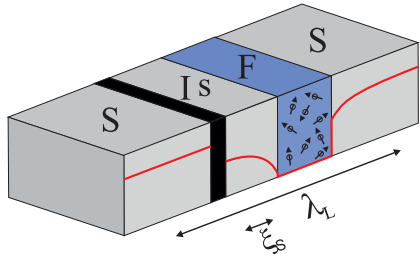


FIG. 1. Schematic design of SIsFS Josephson junction. Solid line demonstrates typical distribution of pair potential Δ along the structure. It reaches bulk values in the S electrodes, is suppressed in the middle s layer and vanishes in the ferromagnetic region F. The characteristic length scales are also marked in the figure: λ_L is the London penetration depth and ξ_S is the coherence length typical for niobium.

SIsFS Josephson devices. We propose a quasiclassical model for a double-barrier Josephson structure in which magnetic and spin states of the F-film in an sFS part of the structure can change the properties and even the ground state of its Sis part. As a result, an external magnetic field may switch the junction from a superconducting to a resistive state or may transform a conventional current-phase relation to an inverted one. We compare the results with experimental data recently obtained for Nb-Al/ AlO_x -Nb-Pd_{0.99}Fe_{0.01}-Nb junctions.

We consider the multilayered structure presented in Fig.1. It consists of two superconducting electrodes 'S' separated by a tunnel barrier 'I', an intermediate thin superconducting film 's' and a ferromagnetic layer 'F'. To describe the supercurrent transport in the structure, we assume that the conditions of a dirty limit are fulfilled for all metals. We also assume that all superconducting films in the structure are made from identical materials, i.e., they can be described by the same critical temperature, T_C , and coherence length, $\xi_S = (D_S/2\pi T_C)^{1/2}$, where D_S is the electronic diffusion coefficient. The tunnel barrier I and the sF and FS interfaces are characterized, respectively, by the following parameters $\gamma_{BI} = R_I \mathcal{A} / \xi_S \rho_S$, $\gamma_{BFS} = R_{FS} \mathcal{A} / \xi_F \rho_F$, and $\gamma = \rho_S \xi_S / \xi_F \rho_F$. Here \mathcal{A} , R_I and R_{FS} are the area and the resistances of the interfaces, $\xi_{S,F}$ and $\rho_{S,F}$ are the coherence lengths and normal state resistivities of S and F materials, respectively. Under the above conditions the Josephson effect in the SIsFS junctions can be described by solving the Usadel equations¹⁹⁻²² with Kupriyanov-Lukichev (KL) boundary conditions²³ at Is, sF and FS interfaces and with the bulk pair potential in the depth of S-electrodes.

The formulated above boundary problem has been solved numerically. The results are summarized in Figs.2-4, where various modes of operation of the structure are defined according to chosen materials and layer thicknesses. These modes are clearly defined by the dependencies of characteristic voltage $I_C R_N$ on thickness of intermediate superconductor, L_s , and ferromagnetic, L_F , layers (see Fig.2 - Fig.4).

Mode (1) in Fig.2. If the thickness of the middle s-electrode, L_s , is much larger than the critical thickness of s layer, L_{sC} , which separates the different modes of operation in SIsFS structures, the pair potential Δ in the s layer is close to that of bulk material. Note that the critical thickness L_{sC} in an sN (sF) bilayer at a given temperature is generally defined as a minimal thickness of an s-layer when superconductivity still exists. In the mode (1) the structure can be considered as a pair of SIs and sFS junctions connected in series. Therefore, the properties of the structure in parameter range (1) are almost independent

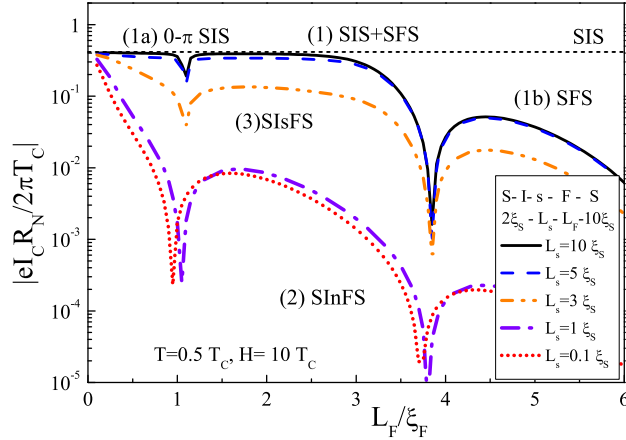


FIG. 2. Characteristic voltage $I_C R_N$ of the SISFS structures versus thickness of the F-layer L_F for different thicknesses of the middle superconducting film L_s at $T = 0.5T_C$. Short-dashed straight line shows the $I_C R_N$ product of the tunnel SIS junction at the same temperature. Interface parameters: $\gamma_{BI} = 1000$, $\gamma_{BFS} = 0.3$ and $\gamma = 1$ at the sF and FS interfaces.

on the thickness L_s and are determined by the junction with smallest critical current. It is seen from Fig.2 that for the given parameter set, $T = 0.5T_C$, $H = 10T_C$, $\gamma = 1$, $\gamma_{BI} = 1000$, $\gamma_{BFS} = 0.3$, the critical thickness of the s layer, L_{sC} , is close to $3\xi_S$.

Mode (1a) in Fig.2. In the ordinary case of $I_{C_{SIS}} \ll I_{C_{sFS}}$, the behavior of the structure coincides with that of conventional SIS junction with one important distinction - the sFS junction can turn the SISFS structure into a π -state. At the same time, other properties like high $I_C R_N$ product and sinusoidal current-phase relation are preserved in the π -state. Therefore the structure can be called switchable $0-\pi$ SIS junction.

Mode (1b) in Fig.2. Another limiting case is realized for large L_F values and high exchange fields H . Namely, the structure transforms into a standard SFS-junction without any influence of tunnel barrier.

Mode (2) in Fig.2. The absence of superconductivity in the s-electrode in the opposite case ($L_s \ll L_{sC}$) leads to formation of the complex -InF- weak link area, where n marks the intermediate s film in the normal state. It results in much smaller critical current value I_C , with the magnitude close to that in well-known SIFS junctions²⁴. The dependence of I_C on the thickness L_s is weak due to large decay length in the n-region with suppressed superconductivity.

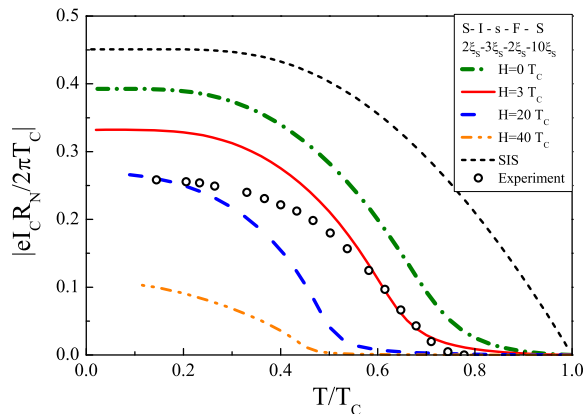


FIG. 3. The temperature dependence of characteristic voltage $I_C R_N$ of SIsFS structure for different values of exchange field H in the F-layer. The short-dashed line demonstrates the dependence characteristic for a conventional tunnel SIS Junction. It is seen how the exchange field H shifts the effective critical temperature T_C^* , corresponding to the switching of the s-layer from the superconducting state to the normal one. The circles show $I_C R_N$ measured in Nb-Al/ AlO_x -Nb-Pd_{0.99}Fe_{0.01}-Nb junctions¹⁶, proving the existence of effective critical temperature T_C^* in these samples.

Mode (3) in Fig.2. Conversely, in the intermediate case ($L_s \approx L_{sC}$) the properties of the structure are extra sensitive to variations of the decay lengths parameters. Within the considered intermediate thickness range the system may transform from the mode (1) to the mode (2). Moreover, in this situation the system is sensitive to the F-layer parameters (thickness L_F and exchange field H), since these parameters control the suppression of superconductivity in the sF bilayer.

This sensitivity allows one to change an operation mode by changing the parameters such as effective exchange field H and temperature T . Note, that depending on the domain structure of a ferromagnet and morphology of the F-film it might be possible to control the effective exchange field H .

Fig.3 demonstrates the temperature dependence of the critical current in the structures with thickness around critical one ($L_{sC} = 3\xi_S$) for different values of exchange field H . These structures are characterized by the existence of the effective critical temperature T_C^* which corresponds to the appearance of superconductivity in middle s-layer and, correspond-

ingly, to an exponential growth of the current. Therefore, T_C^* may significantly shift during remagnetization of the system (due to changing of H , as pointed out above). Thus, system can exist either in the superconducting or in the normal state depending on the history of the application of a magnetic field. On the other hand, from point of view of practical applications, the 0- π SIS mode (1a) seems more relevant.

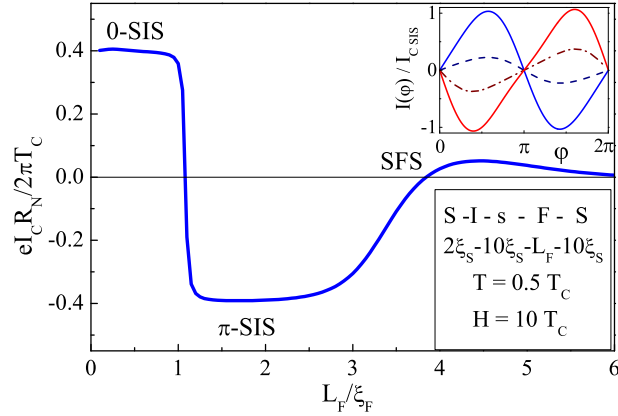


FIG. 4. The dependence of characteristic voltage $I_C R_N$ on F-layer thickness L_F in the SISFS structure with the s-layer in the superconducting state. Inset shows the current-phase relation in the vicinity of the first 0 – π transition. Switching from 0 to π state in the mode (1a) preserves the value of critical current I_C as well as characteristic voltage $I_C R_N$.

Fig.4 demonstrates that change of F-layer thickness L_F leads to 0- π transition. The system can be switched into a π -state keeping the value of $I_C R_N$ product, i.e., Josephson frequency, on the level characteristic for tunnel SIS junctions. Moreover, it should be noted that this property of the considered structure is unique. In the conventional SFS devices in order to reach the π -state it is necessary to realize either $L_F \gtrsim (2 - 3)\xi_F$ or very large values of the $\gamma_{BFS} \gg 1$ parameter at the SF interfaces. In both cases the $I_C R_N$ product in the π -state is strongly reduced^{20-22,24}.

External magnetic field. In the parameter range when SISFS junction is in (1a) mode and far from the 0 – π transition, current-phase relation has a sinusoidal form, $I(\varphi) \approx I_{SI_s} \sin \varphi$. To calculate the dependence of I_C from external magnetic field, H_{ext} , we may use the standard Fraunhofer expression,

$$I_C(H_{ext}) = I_{C0} \left| \frac{\sin(\pi\Phi/\Phi_0)}{\pi\Phi/\Phi_0} \right|, \quad (1)$$

where

$$\Phi = W |L_{eff}H_{ext} + L_F H_0 N(n_{\uparrow} - n_{\downarrow})| \quad (2)$$

is magnetic flux inside of SIFS junction, Φ_0 is flux quantum, $L_{eff} = 2\lambda_L + L_s + L_F + L_I$, λ_L is London penetration depth of S electrodes, L_I is thickness of I layer, N is the full number of clusters, $n_{\uparrow,\downarrow} = N_{\uparrow,\downarrow}/N$ are the concentrations of clusters in the F layer oriented parallel (N_{\uparrow}) or antiparallel (N_{\downarrow}) to the direction of H_{ext} in the saturation region and H_0 is an average magnetic field generated by a single magnetic cluster. In our simple model, H_0 is assumed to be a constant, while n_{\uparrow} and n_{\downarrow} are functions of H_{ext} . We assume further that the probability density $p(H_{ext})$ of a flip of a cluster in H_{ext} is described by a Gaussian distribution

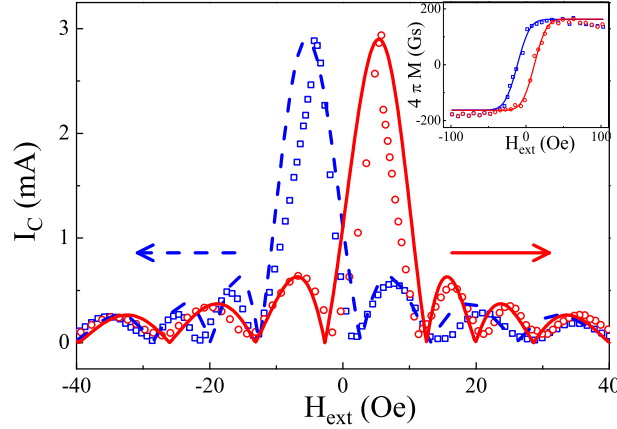


FIG. 5. Experimental dependence¹⁶ of critical current I_C versus increasing (open circles) and decreasing (open squares) external magnetic field H_{ext} . Solid and dashed lines present the microscopic fitting of the data. Inset shows the theoretical and experimental magnetization loops versus external magnetic field H_{ext} .

$$p(H_{ext}) = (\sqrt{2}/\sqrt{\pi}\delta) \exp \left[- (H_{ext} - H^*)^2 / 2\delta^2 \right], \quad (3)$$

where H^* is the value of magnetic field, at which the flip of a cluster takes place. The expectation, H^* , and the standard deviation, δ , in (3) are independent on H_{ext} values. These parameters, as well as H_0N product (i.e. saturation of the magnetization magnitude) in Eq.(2) can be found by fitting the magnetization curve $4\pi M(H_{ext})$.

We apply this model to explain the data experimentally observed in Ref.¹⁶ in SIFS structures having cross-section area $10 * 10 \mu\text{m}^2$ and F layer thickness 14 nm. Figure 5

demonstrates the experimental dependencies of critical current I_C versus increasing (open circles) and decreasing (open squares) external magnetic field H_{ext} . Solid and dashed lines present the microscopic fitting of the data. From hysteretic dependencies of F layer magnetization shown in insert in Fig. 5 we get $H^* \approx 11.4$ Oe, $\delta \approx 13$ Oe and H_0N product ≈ 163 G. Remaining fitting parameters can be set from the current magnitude in the main maximum $I_{C0} \approx 2.9$ mA and from the difference between zeros of $I_c(H)$ dependence in the saturation region, where oscillation period depends entirely on the effective length of structure $L_{eff} \approx 150$ nm.

The initial strong magnetic field $H_{ext} = -\infty$ remagnetize all clusters of F layer into the homogeneous state $n_{\downarrow}(H_{ext}) = 1$. Gradual growth of the external field provides the conventional Fraunhofer pattern (solid line) with expected maximum at the positive value H_{ext} corresponding to zero flux $\Phi = 0$. However, the clusters start to flip around the point $H_{ext} = H^*$, $n_{\uparrow}(H_{ext}) = \int_{-\infty}^{H_{ext}} p(H'_{ext}) dH'_{ext}$. As a result, the period of Fraunhofer oscillations decreases. Similar situation takes place during field sweeping in the opposite direction (dashed line), from large positive to negative values. The densities $n_{\uparrow}(H_{ext})$ and $n_{\downarrow}(H_{ext}) = 1 - n_{\uparrow}(H_{ext})$ can be described by the expression, $n_{\uparrow}(H_{ext}) = 0.5 (1 + erf((H_{ext} \mp H^*)/\sqrt{2}\delta))$, for forward and backward remagnetizations, respectively. Here $erf(x)$ is the error function.

In this paper we have demonstrated a number of unique properties of SISFS Josephson junctions. These structures exhibit a large $I_C R_N$ product in the π state comparable to that in SIS tunnel junctions commonly used in SFQ devices. Moreover, the whole structure behaves as a single junction with respect to an external magnetic field H_{ext} . Based on that, we have developed simple model describing the behavior of the critical current in these junctions in external field H_{ext} taking into account remagnetization of the F-layer. The model explains asymmetric Fraunhofer oscillations $I_C(H_{ext})$ in Nb-Al/AlO_x-Nb-Pd_{0.99}Fe_{0.01}-Nb junctions reported in¹⁵⁻¹⁷. These effects provide the possibility to realize magnetic memory compatible with energy-efficient SFQ digital circuits²⁵ with high switching speed.

This work was supported by the Russian Foundation for Basic Research, Russian Ministry of Education and Science, Dynasty Foundation, Scholarship of the President of the Russian Federation and Dutch FOM.

REFERENCES

- ¹S. Oh, D. Youm, and M. Beasley, *Appl. Phys. Lett.* **71**, 2376 (1997).
- ²L. R. Tagirov, *Phys. Rev. Lett.* **83**, 2058 (1999).
- ³R. Held, J. Xu, A. Schmehl, C.W. Schneider, J. Mannhart, and M. Beasley, *Appl. Phys. Lett.* **89**, 163509 (2006).
- ⁴V.V. Ryazanov, *Physics - Uspekhi* **42**, 825 (1999).
- ⁵V.V. Ryazanov, V.A. Oboznov, A.Yu. Rusanov, A.V. Veretennikov, A.A. Golubov, J. Aarts, *Phys. Rev. Lett.* **86**, 2427 (2001).
- ⁶F. S. Bergeret, A. F. Volkov, and K. B. Efetov, *Phys. Rev. Lett.* **86**, 3140 (2001).
- ⁷A. A. Golubov, M. Yu. Kupriyanov, and Ya. V. Fominov, *Pis'ma v ZhETF* **75**, 223 (2002) [*JETP Letters* **75**, 190 (2002)].
- ⁸A. F. Volkov, F. S. Bergeret, and K. B. Efetov, *Phys. Rev. B* **64**, 134506 (2001).
- ⁹M. Houzet and A. I. Buzdin, *Phys. Rev. B* **76**, 060504(R) (2007).
- ¹⁰T. Yu. Karminskaya and M. Yu. Kupriyanov, *Pis'ma v ZhETF* **85**, 343 (2007) [*JETP Lett.* **85**, 286 (2007)].
- ¹¹T. Yu. Karminskaya, M. Yu. Kupriyanov, and A. A. Golubov, *Pis'ma v ZhETF* **87**, 657 (2008) [*JETP Lett.* **87**, 570 (2008)].
- ¹²G. B. Halasz, M. G. Blamire, and J. W. A. Robinson, *Phys. Rev. B* **84**, 024517 (2011).
- ¹³T. S. Khaire, M. A. Khasawneh, W. P. Pratt, Jr., and N. O. Birge, *Phys. Rev. Lett.* **104**, 137002 (2010).
- ¹⁴V. V. Bol'ginov, V. S. Stolyarov, D. S. Sobanin, A. L. Karpovich, and V. V. Ryazanov, *Pis'ma v ZhETF* **95**, 408 (2012) [*JETP Lett.* **95**, 366 (2012)].
- ¹⁵T. I. Larkin, V. V. Bol'ginov, V. S. Stolyarov, V. V. Ryazanov, I. V. Vernik, S. K. Tolpygo, and O. A. Mukhanov, *Appl. Phys. Lett.* **100**, 222601 (2012).
- ¹⁶I. V. Vernik, V. V. Bol'ginov, S. V. Bakurskiy, A. A. Golubov, M. Y. Kupriyanov, V. V. Ryazanov, O. A. Mukhanov, *IEEE Trans. Appl. Supercond.* **23**, 1701208 (2013).
- ¹⁷V. V. Ryazanov, V. V. Bol'ginov, D. S. Sobanin, I. V. Vernik, S. K. Tolpygo, A. M. Kadin, O. A. Mukhanov, *Physics Procedia* **36**, 35 (2012).
- ¹⁸L. S. Uspenskaya, A. L. Rahmanov, L. A. Dorosinskiy, A. A. Chugunov, V. S. Stolyarov, O. V. Skryabina, and S. V. Egorov, *Pisma v ZhETF* **97**, 176 (2013) [*JETP Lett.* **97**, 155 (2013)].

- ¹⁹K. D. Usadel, Phys. Rev. Lett. **25**, 507 (1970).
- ²⁰A. A. Golubov, M. Yu. Kupriyanov, E. Il'ichev, Rev. Mod. Phys. **76**, 411 (2004).
- ²¹A. I. Buzdin, Rev. Mod. Phys. **77**, 935 (2005).
- ²²F. S. Bergeret, A. F. Volkov, K. B. Efetov, Rev. Mod. Phys. **77**, 1321 (2005).
- ²³M. Yu. Kupriyanov and V. F. Lukichev, Zh. Eksp. Teor. Fiz. **94**, 139 (1988) [Sov. Phys. JETP **67**, 1163 (1988)].
- ²⁴A. S. Vasenko, A. A. Golubov, M. Yu. Kupriyanov, and M. Weides, Phys. Rev. B **77**, 134507 (2008).
- ²⁵O.A. Mukhanov, IEEE Trans. Appl. Supercond. **21**, 760 (2011).